CHAPTER 3

Evidence of surface and bulk magnetic ordering in Fe and Mn doped $Bi_2(SeS)_3$ topological insulator

3.1 Introduction

Topological insulators (TIs) are introduced as a new class of quantum matter, which are characterized by linearly dispersed spin-polarized gapless surface states within the bulk band gaps[4], [28], [37]–[40]. The surface state is protected by time-reversal symmetry, which leads to a variety of effects, such as the Quantum spin Hall effect, a large value of Magneto-resistance [41], [42]. Such exotic properties of TIs make them the future of next-generation spintronic devices[43], [44].

By breaking time-reversal symmetry, the surface state of TIs can be modified remarkably. However, the time-reversal symmetry (TRS) can be broken by introducing magnetism in TIs, which leads to opening a finite energy gap at the Dirac point, inevitably very important for potential device applications[41], [42], [45]. The origins of such strongly coupled magnetism in TIs are still under debate. Checkelsky et al.[46] reported the suppression of ferromagnetism in Mn-doped $Bi_2Te_{3-y}Se_y$ by increasing carrier densities, suggesting a Dirac-fermion-mediated origin for the surface ferromagnetism in TIs. In contrast, for the long-range ferromagnetic order in a Cr-doped $(Bi_ySb_{1-y})_2Te_3$ film, Chang et al.[47] demonstrated independence of Curie temperature (T_C) with carrier density. However, in magnetic TI systems, ferromagnetic moments can be developed through two major mechanisms: the van Vleck mechanism and the Ruderman-Kittel-Kasuya-Yosida (RKKY) coupling [48]–[50]. In the case of the van Vleck mechanism, the magnetic ions are directly coupled through the local valence electrons due to their large spin susceptibility. Obviously, this bulk ferromagnetism is independent of the carrier density [49]. On the other hand, neighboring magnetic ions can also be coupled through the mediation of conduction carriers and this kind of coupling is referred to as the carrier-mediated RKKY interaction [51]–[53].

Kou et al. [54] have reported the presence of both the hole-mediated RKKY coupling and the carrier-independent bulk van Vleck magnetism in the Cr-doped $(Bi_xSb_{1-x})_2Te_3$ thin films from the top-gate-modulated magnetotransport measurements. However, there still remains ambiguity regarding the interplay between the TI surface state and magnetic ordering. Moreover, the 3d transition metals doped topological insulators have been extensively studied in which Bi_2Se_3 is the most depictive second-generation TIs because this shows a sufficiently large band gap of 0.3eV [39], [55]. It will be very intriguing to find out the correlation between topological surface state and magnetism in the TIs upon magnetic impurity doping [41], [56]. The presence of ferromagnetism in the magnetic TIs generally suggests the existence of the Anomalous Hall Effect (AHE). Interestingly, we didn't observe any signature of AHE in the present investigation, which is consistent with those of reported results in which the AHE is absent despite compelling evidence for ferromagnetism[41], [57]–[59].

In the present work, we have investigated the origin of bulk and surface magnetism by doping 3d-transition-metal impurities (Mn and Fe) in $Bi_2Se_{3-y}S_y$ by measuring magnetization and angle-resolved photoemission spectroscopy (ARPES). We have also demonstrated the coexistence of both surface and bulk magnetizations in $Bi_{2-x}Fe_xSe_{3-y}S_y$.Moreover, we have also performed a theoretical calculation to understand the mechanism in a better way, and it supports our experimental results. We have chosen $Bi_2Se_{3-y}S_y$ as in another study [22] we have shown that Sulphur (S) incorporation in the Bi_2Se_3 introduces electrons by *n*-type antisite disorder, which may help in coupling between magnetic ions via those itinerant electrons.

3.2 Experimental Details

The single crystals of $Bi_{2-x}Fe_xSe_{2.79}S_{0.21}$ and $Bi_{2-x}Mn_xSe_{2.79}S_{0.21}$were synthesized by the modified Bridgeman method, as has been reported elsewhere[60]. The prepared single crystals were characterized by X-ray diffraction [figure 3.1] for phase identification. The X-ray diffracted beam direction showed only along the (*00l*) plane with the space group of Bi_2Se_3 ($R\bar{3}m$) suggesting the sample is growing along c-axis [60]. The Lattice parameters have been determined using Rietveld refinement of powder XRD. We have performed the magnetic measurements by using the Quantum Design SQUID magnetic properties measurement system (MPMS). Hall effect measurement was carried out by using the physical properties measurement system (PPMS). Angle-Resolved Photo Emission Spectroscopy (ARPES) measurement has been done with a µ-Laser ARPES system with a photon energy of 6.3 eV at HiSOR, Hiroshima University, Japan, which confirmed the topological surface state of the prepared samples at 20K. All the samples were cleaved in-situ at 30K along the c-axis in an ultrahigh vacuum (~5×10^{-11})Torr [61]. A very clean mirror-like surface was obtained after cleaving. The samples are found to be stable for more than two days in the UHV chamber.

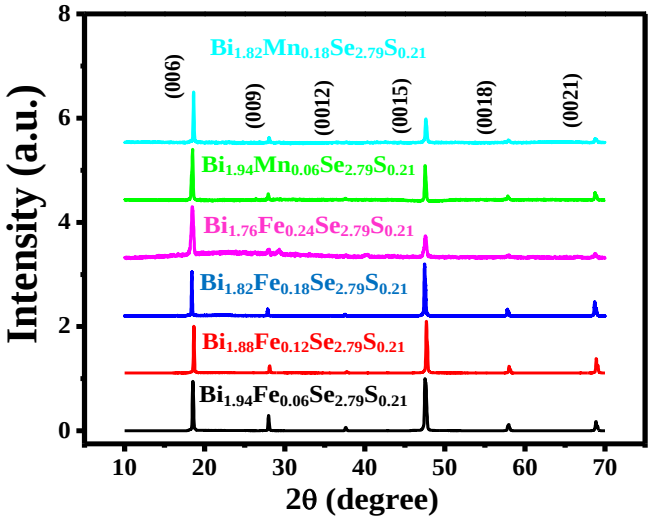

Figure 3.1: XRD pattern for all the prepared single crystal samples cleaved along (*00l*) plane.

3.3 Results and discussion

3.3.1 Experimental study

In order to determine the mobility and carrier concentration of our Fe-doped and Mn-doped series, we have performed Hall measurement at different temperatures. The variation of Hall resistivity as a function of magnetic field (H) at different temperatures is shown in figure 3.2. For $Bi_{2-x}Fe_xSe_{2.79}S_{0.21,}$ the Hall data shows a negative slope, which indicates that charge carriers are electrons while for $Bi_{2-x}Mn_xSe_{2.79}S_{0.21}$ slope changes from negative (pure Bi_2Se_3) to positive showing that carriers are tuned from n-type to p-type for the entire temperature range of measurement which is also consistent with the ARPES results (discussed below). The estimated values of mobility are well-matched with the reported values [62], [63], which is shown in Table-1. On increasing doping percentage, the value of mobility is decreased because of increment in scattering centers. Furthermore, the increase of carrier concentration with temperature suggests the increase of the bulk contribution with temperature.

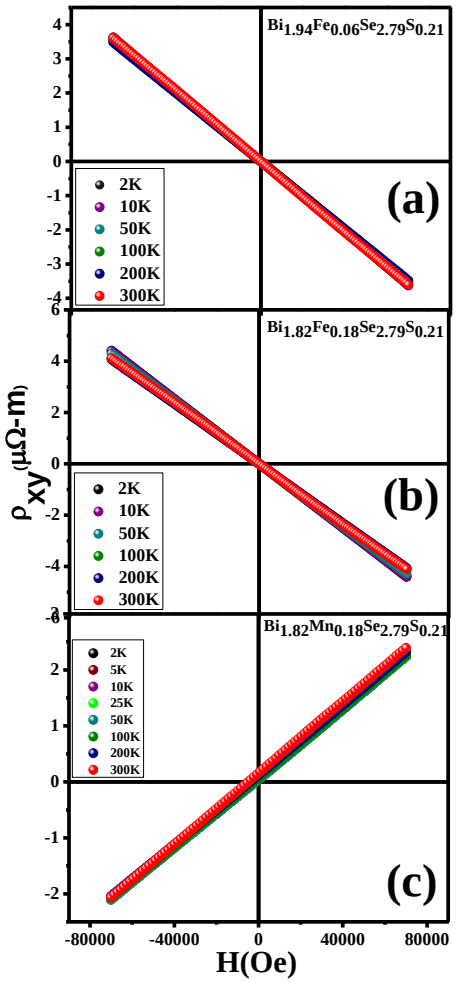

Figure 3.2: The variation of Hall resistivity as a function of applied magnetic field (a) x=0.06, (b) x=0.18 for $Bi_{2-x}Fe_xSe_{2.79}S_{0.21}$, (c) 0.18 for $Bi_{2-x}Mn_xSe_{2.79}S_{0.21}$ at different temperatures.

In order to investigate the surface state and electronic structure in detail, we have performed ARPES measurement of Fe and Mn doped systems. As we dope magnetic impurity Fe in S-doped Bi_2Se_3, we expect a gap opening at the Dirac point of Topological surface state [27]. Figure 3.3 (a) and 3.3 (b), respectively for x=0.06 and x=0.12 suggest the presence of surface state in both the samples. TSS starts to disappear in x=0.18 and in x=0.24 it almost disappears. Figure 3.3 illustrates the measured band structure of all the samples in which Dirac Point (DP) lie below the Fermi energy with a certain band gap and gives a clear

indication of the existence of the surface state. Position of DP and band gap of all the samples is given in Table-1. As we increase the doping content, a clear gap opening is observed which is correlated with the ferromagnetic ordering (will be discussed later). The Fermi energy lifts upward on increasing magnetic doping which shows the n-type behaviour of the series which is consistent with the Hall data.

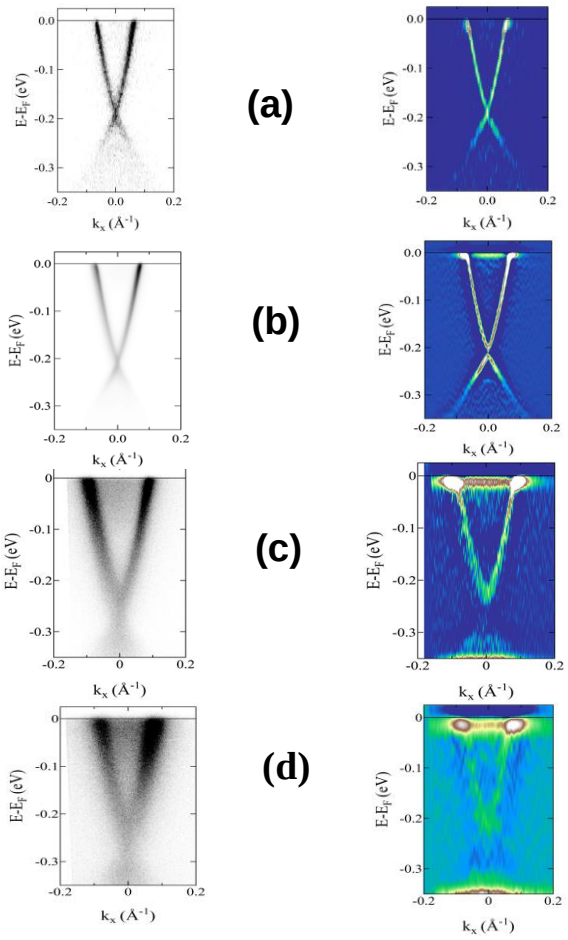

Figure 3.3: ARPES spectra for (a) x=0.06, (b) x=0.12, (c) x=0.18, and (d) 0.24 of $Bi_{2-x}Fe_xSe_{2.79}S_{0.21}$.

Table-3.1: The obtained different parameters from ARPES and Hall effect measurements.

Composition $Bi_{2-x}Fe_xSe_{3-y}S_y$	**Band Gap (ARPES)**	**Position of DP (ARPES)**	**Bulk carrier concentration (n_b) (2K)**	**Mobility (μ) (2K)**
x=0.06	18 meV	-185 meV	$1.20\times10^{19}/cm^3$	3262 $cm^2/V.S$
x=0.12	25 meV	-210 meV	$1.06\times10^{19}/cm^3$	2049 $cm^2/V.S$
x=0.18	55 meV	-250 meV	$9.86\times10^{18}/cm^3$	879 $cm^2/V.S$
x=0.24	80 meV	-270 meV	$7.02\times10^{18}/cm^3$	1685 $cm^2/V.S$
$Bi_{2-x}Mn_xSe_{3-y}S_y$ x=0.12	-	-	$1.16\times10^{19}/cm^3$	1024 $cm^2/V.S$
x=0.18	-	-	$1.96\times10^{19}/cm^3$	1770 $cm^2/V.S$

To further check the surface and bulk contribution in magnetic ordering, we changed the dopant from Fe to Mn, with one less valence electron than Fe (figure 3.4). Indeed, Mn dopants other than inducing magnetic moment, also introduces holes into the system (Supported by Hall data). The measurements on x=0.12 sample show E_F lying just inside the surface state band gap (figure 3.4 (a)). By comparing the leading edge at the G point to E_F, we found a slight difference, indicating a surface state band (SSB) Dirac gap with very low value (figure 3.4 (b)). On the other hand, x=0.18 sample does not show any band gap (figure 3.4 (d)).

To understand the magnetic state of $Bi_{2-x}Fe_xSe_{2.79}S_{0.21}$, in figure 3.5 we have shown magnetization as a function of magnetic field (M-H) in the temperature range (2K<T<300K). From M-H curves, it is clear that a giant ferromagnetic (FM) ordering with broad hysteresis is present in the whole series as well as in the entire temperature range from 2K to 300K. For further confirmation, we also plotted the Arrott plots for the samples which also confirm the presence of ferromagnetic ordering in the samples [in figure 3.6]. We have also performed magnetization vs. temperature (M-T) measurements above room temperature is shown in figure 3.6, which further suggest the presence of magnetic ordering

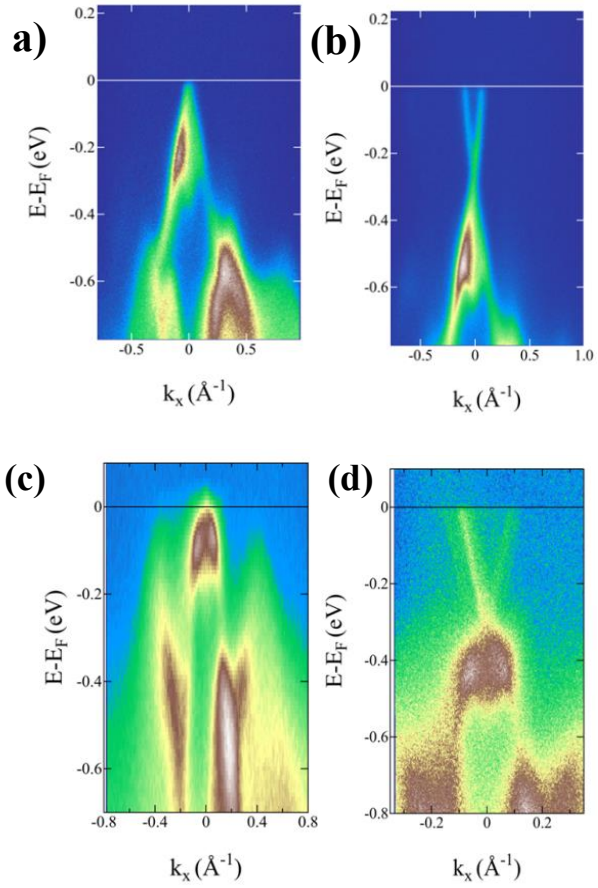

Figure 3.4: ARPES spectra for (a), (b) for x=0.12, (c), (d) for x=0.18 of $Bi_{2-x}Mn_xSe_{2.79}S_{0.21}$.

above room temperature. The Magnetic Force Microscopy (MFM) images [in figure 3.6] of the samples also show the room temperature FM ordering. The most intriguing fact is the observation of ferromagnetic ordering even at room temperature for the whole series of samples which is not consistent with the reported FM TIs where magnetic ordering is observed at very low temperature[30], [64], [65]. Such a giant ferromagnetism is supposed to open a gap at Dirac point. From figure 3.3, it is clear that the gap opening exists at the Dirac point for all the doping concentrations which varies from 18 meV to 80 meV. The gap opening is also increased on increasing magnetic impurity [discussed in ARPES part]. The value of the band gap with the doping concentration is presented in Table-1 which is

consistent with the magnetic data. Based on the present results, it is clear that particularly, when the Fermi level (E_F) is away from the surface band gap for x=0.06 and 0.12 Fe doped samples (as is clear from the ARPES) and close to the bulk conduction band, coercivity (H_c) value is ~7000 Oe. On the contrary, with increasing temperature as the E_F moves towards valence band[66] H_c decreases, and finally approaches to its minimum value around 2650 Oe at room temperature. It is worthwhile to mention that as the temperature increases the bulk state dominates over surface state by increasing the carrier concentration which is clear from the Hall study (discussed above). Moreover, one may expect excessive Fe atoms weaken the surface state which is also clear from the ARPES result for the x=0.18 and 0.24 Fe doped samples. However, it is observed that H_c value for x=0.18 and 0.24 is almost equal to that of the lower doped samples (x=0.06 and 0.12 Fe doped) throughout the whole temperature range. Furthermore, for all the samples at 300 K the H_c value is more or less equal. All these suggest that when surface state is diminished the H_c value is carrier independent. This further suggests that not only the surface state but the bulk state is also responsible for inducing ferromagnetism in Fe doped $Bi_2(SeS)_3$ and this bulk induced magnetism is carrier independent whereas the surface induced FM is carrier dependent. The surface induced magnetic ordering in TIs can be attributed to the RKKY interaction [27], [67], [68]. Therefore, RKKY interaction is gradually suppressed as the surface state becomes weaker with increase of temperature. On the other hand, in the region where E_F is far below the bulk conduction band, the presence of low H_c supports the existence of additional ferromagnetic contribution where the robust magnetic order is formed without the assistance of the itinerant carriers. This bulk ferromagnetism is attributed to the bulk van Vleck ferromagnetism [47], [49], [69].

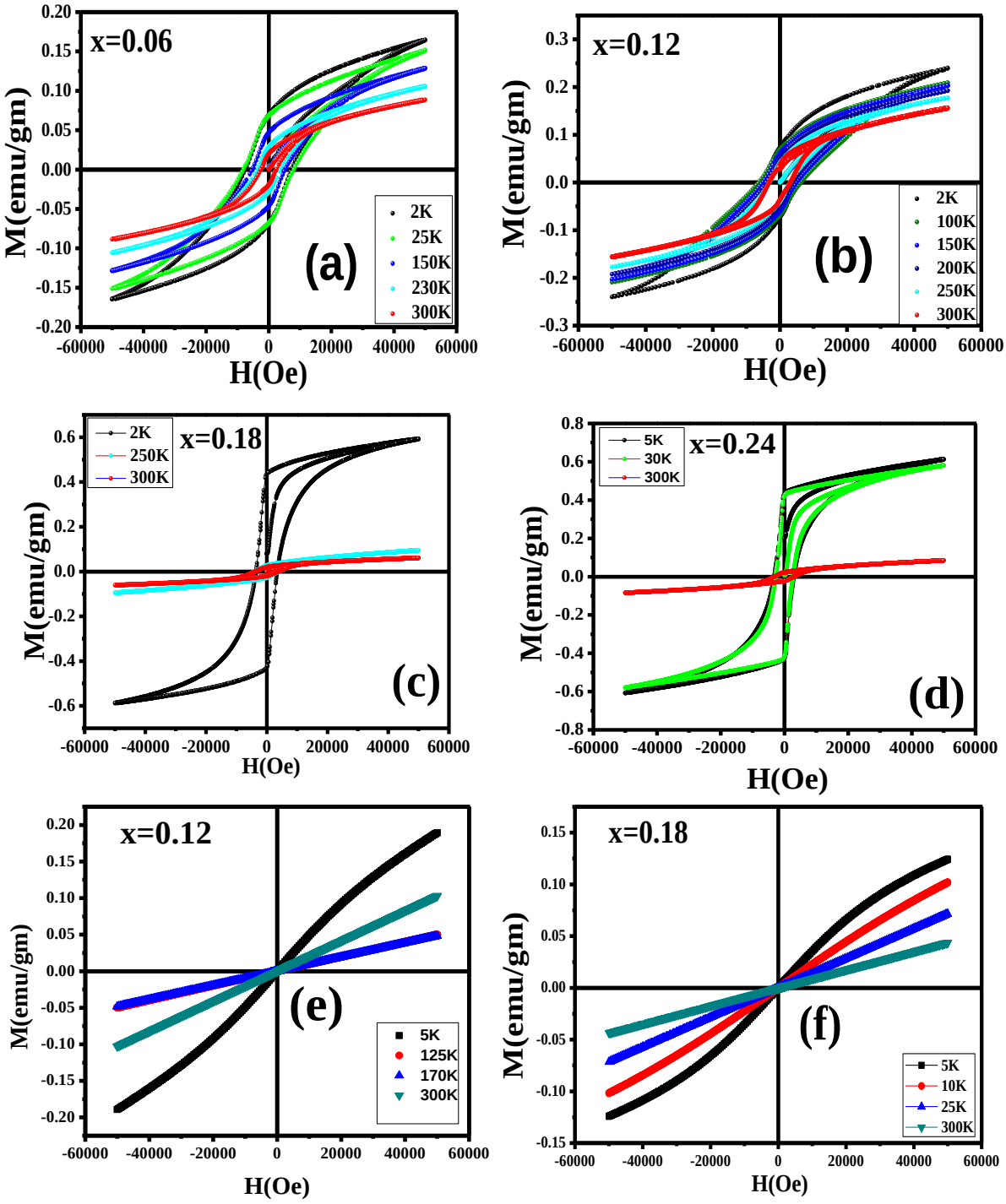

Figure 3.5: Magnetization (M) as a function of applied magnetic field (H) of $Bi_{2-x}Fe_xSe_{2.79}S_{0.21}$ with (a) x=0.06, (b) x=0.12, (c) x=0.18, (d) 0.24 and of $Bi_{2-x}Mn_xSe_{2.79}S_{0.21}$ for (e) x=0.12, (f) x=0.18 at different temperatures.

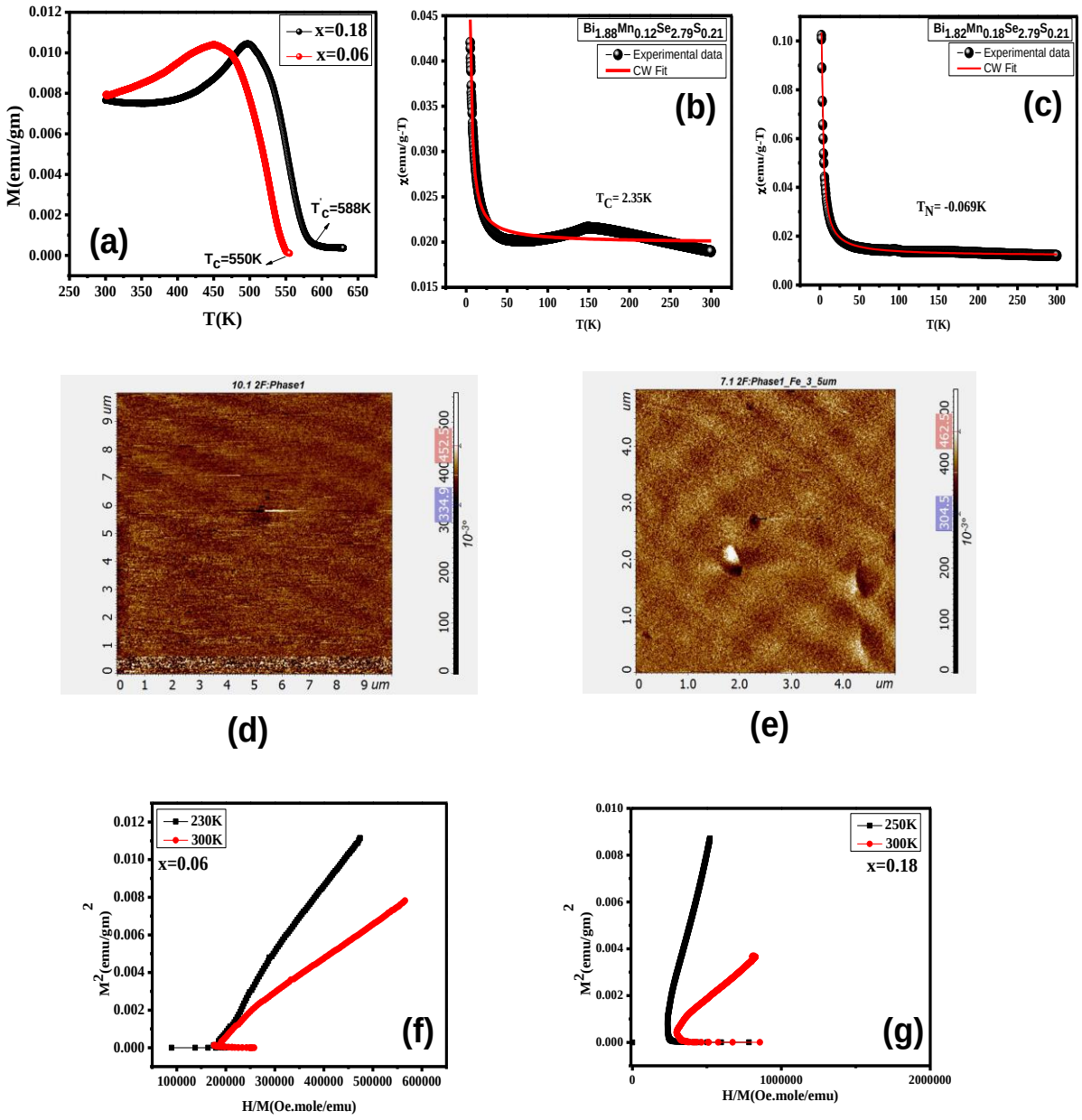

Figure 3.6: (a) magnetization vs. temperature (M-T (ZFC)) curve of $Bi_{2-x}Fe_xSe_{2.79}S_{0.21}$. The Variation of Magnetic Susceptibility as a function of temperature (b) $Bi_{1.88}Mn_{0.12}Se_{2.79}S_{0.21}$ (c) $Bi_{1.82}Mn_{0.18}Se_{2.79}S_{0.21}$ (d) MFM image of $Bi_{2-x}Fe_xSe_{2.79}S_{0.21,}$ for x=0.06 and (e) for x=0.18 (f) Arrott plot of $Bi_{2-x}Fe_xSe_{2.79}S_{0.21,}$ for x=0.06 and (g) x=0.18.

As more Fe is doped in the TI system, the bulk van Vleck magnetism is expected to become stronger due to the enhanced out-of-plane magnetic moments from the Fe ions.

Under such circumstance, the electron-mediated RKKY interaction becomes diminished or even completely suppressed, leaving only the bulk van Vleck responses in heavily Fe-doped TI samples [47], [54], [69]. As has been mentioned in the present case with variation of temperature the H_c remains constant in these heavily doped samples. This carrier independent bulk ferromagnetism further supports the existence of bulk van Vleck ferromagnetism. Accordingly, we may infer that the observed ferromagnetism in Fe doped $Bi_2(SeS)_3$ is due to the coexistence of both electron-mediated RKKY and van Vleck mechanisms.

The M(H) curve for $Bi_{2-x}Mn_xSe_{2.79}S_{0.21}$ at different temperatures is shown in figure 3.5 (e) and (f). At low temperature (5K), a clear signature of non-linearity in M(H) curve is observed for both the samples. There is no sign of saturation in M(H) curve upto 5T, which might be an indication of presence of AFM ordering for both the samples. However, for x=0.12 sample deviation from linearity is slightly larger than that from the x=0.18 indicating also the existence of FM ordering in x=0.12. On increasing temperature, both x=0.12 and x=0.18 show paramagnetic state up to room temperature. We have also checked the magnetic ordering by fitting the M(T) data with the Curie-Weiss law [Figure 3.6 (b) and (c)]. It is found that for x=0.12 Mn doped sample the Curie-Weiss temperature is positive suggesting FM ordering and for x=0.18 sample it is negative suggesting AFM ordering. The AFM coupling was also observed in many TIs such as Cr and Gd doped TIs as well as in layered magnetically doped BiTeI[70]–[72]. $MnBi_2Te_4$ is recently discovered magnetically-ordered AFM topological insulator which shows A-type AFM [73]. For the case of Mn doped $Bi_2(SeS)_3$ the observed surface gap from ARPES also suggests the existence of a ferromagnetic order (along with AFM) of the x=0.12 Mn dopants on the surface. Moreover, it has already been mentioned that with increase of temperature surface state is diminished and bulk state

dominates. Furthermore, with further increase of Mn doping content the AFM ordering is observed both from M(T) and M(H) data supporting the absence of surface gap observed in ARPES[73], [74]. This further supports existence of hole mediated RKKY mechanism in Mn doped $Bi_2(SeS)_3$ system. Therefore, present study suggests that Fe is doped both in surface and bulk whereas Mn is doped in surface only.

3.3.2 Theoretical study

In order to further find out the origin the magnetic ordering in Fe and Mn doped $Bi_2(SeS)_3$ the first-principle density functional theory calculations are performed using the Quantum Espresso package [75]–[77], with pseudopotentials from the PSLibrary[78]. The plane-wave method is used with ultra-soft pseudopotentials[79] and Perdew-Burke-Ernzerhof-type generalized gradient approximation (GGA)for exchange-correlation functional[80].A plane-wave energy cutoff of 80 eV and a charge density cutoff of 640 eVis used in all the calculations. A gamma-centered 5x5x2 mesh of special k points is adopted for integrations over the Brillouin zone. The cutoff and k-mesh values are found after convergence with respect to the total energy. Unless mentioned otherwise, spin-orbit coupling (SOC) is taken into account in all calculations. Crystalline Bi_2Se_3 has a rhombohedral structure and its unit cell is composed of three weakly coupled quintuple layers (QLs). We employ a 2x2x1 supercell containing 24 Bi and 36 Se atoms for our calculations. For doped system, 2 Bi atoms are replaced with Mn atoms and 4 Se atoms are replaced with S atoms (for x=0.18 doping). We have used the lattice constants obtained from our XRD data. For the doped compounds, the internal coordinates of all atoms are relaxed until the residual forces on each atom are less than 0.02 eV/Angstrom.

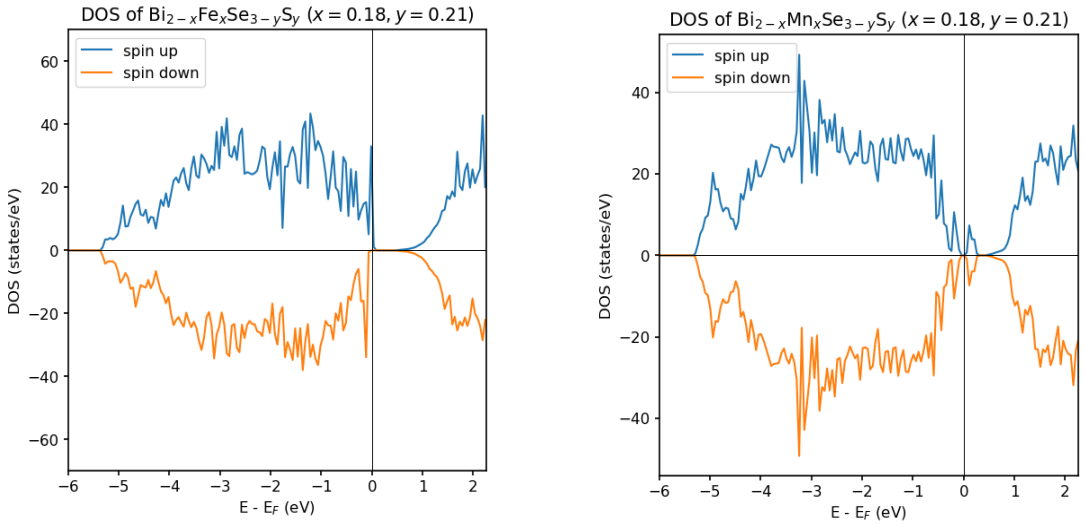

(a) (b)

Figure 3.7: Density of States (DOS) from DFT Calculation for (a) $Bi_{1.82}Fe_{0.18}Se_{2.79}S_{0.21}$ and (b) $Bi_{1.82}Mn0_{.18}Se_{2.79}S_{0.21}$.

The DOS of up and down spins are colored in blue and Red. From figure 3.7, we can see that DOS of two spin states is perfectly equal and shows symmetric DOS indicating the absence of FM ground state. We have also obtained minimum total energy for AFM state with the energy value -4593.2327 Ry while for ferromagnetic state the value of total energy is -4593.2286Ry. The total energy value also supports AFM ground state for Mn doped system which is consistent with the magnetic measurement (at low T). Furthermore, the Fe doped sample shows asymmetric DOS (figure 3.7 (a)) for spin up and spin down suggesting the robust ferromagnetic ordering. Therefore, theoretical result is consistent with that of experiment.

3.4 Conclusion:

In conclusion, the Hall effect, angle resolved photoemission spectroscopy (ARPES) and magnetization of $Bi_{2-x}M_x(SeS)_3$ (with M=Fe, Mn) have been investigated. ARPES study

shows that with increase of Fe doping surface band gap gradually increases. With Mn doping initially the surface band gap is opened up slighty but with further increase of doping content the band gap is closed. In Fe doped $Bi_2(SeS)_3$ the presence of both the electron-mediated RKKY coupling and carrier-independent van Vleck magnetism have been demonstrated. On the other hand, in Mn doped sample hole-mediated RKKY coupling is observed. The result from DFT calculation also supports this experimental interpretation. Furthermore, both ARPES and magnetic studies indicate that surface magnetic ordering may or may not break the time reversal symmetry (TRS) whereas bulk magnetic ordering breaks the TRS. This observation suggests the usefulness of TI-based device for spintronics.